Journal of Gerontology: BIOLOGICAL SCIENCES
Cite journal as: J Gerontol A Biol Sci Med Sci. 2010 November;65A(11):1157–1164
doi:10.1093/gerona/glq141

Advance Access published on August 26, 2010

Decrease in Mitochondrial Function in Rat Cardiac Permeabilized Fibers Correlates With the Aging Phenotype

Hélène Lemieux,[1,2] Edwin J. Vazquez,[1,2] Hisashi Fujioka,[1,2] and Charles L. Hoppel[1,2]

[1]Center for Mitochondrial Disease and [2]Department of Pharmacology and Medicine, Case Western Reserve University, Cleveland, Ohio.

Address correspondence to Charles L. Hoppel, Center for Mitochondrial Disease, Department of Pharmacology, Case Western Reserve University, 10900 Euclid Avenue, Cleveland, OH 44106. Email: charles.hoppel@case.edu

We measured the loss of cardiac mitochondrial function related to aging in males of three rat strains presenting with different longevity and aging phenotypes: the Fischer 344 (F344), the Brown Norway (BN), and the hybrid F344×BN. The F344 rat has a short life span and a ~45% decrease in coupled mitochondrial oxidation in the cardiac permeabilized fibers from the old rats compared with the young rats. Citrate synthase activity in the permeabilized fibers (mitochondrial content) did not change significantly with aging. The BN live longer compared with the F344 and have a 15%–18% loss of mitochondrial respiration in the aged rats compared with the young rats. The differences are not significant. In hybrids, more resistant to aging than are the BN and the F344, mitochondrial function is preserved during aging. The difference in longevity of the different strains is correlated with mitochondrial dysfunction in the heart, suggesting the importance of mitochondria in cardiac aging.

Key Words: Aging—Mitochondrial—Oxidative phosphorylation—Rat—Strains.

Received May 11, 2010; Accepted July 14, 2010

Decision Editor: Rafael de Cabo, PhD

AGING involves a progressive decline in physiological function, leading to an increased rate of disease (1,2), including cardiovascular disease (3,4). The reason why certain human beings and animals exhibit an exceptional longevity is that they appeared to be immune to significant diseases, including cardiovascular disease (5,6). Siblings of centenarians showed a 50% decrease in prevalence of hypertension, myocardial infarction, and stroke compared with age-matched controls (6), increasing their chances of living over 100 years by a factor of 8- to 17-fold compared with the general population (6,7).

Similarly, in animal models, variability in aging phenotype previously has been shown to occur between strains (8) and even substrains (9) within a species. Among rats, the Fisher 344 (F344) strain has been well recognized for aging studies because it shows severe age-related pathology and a shorter life expectancy compared with other rat models (10). Other rats that have been used for aging study include the Brown Norway (BN) and the hybrid Fisher 344×Brown Norway (F344×BN), whose life span is longer than that of the F344 (10).

The longevity phenotype is likely to involve adaptive strategies at the molecular and cellular levels, conferring protection against basic mechanisms of aging and/or age-related illnesses (11). Previous studies have pointed out two genes associated with longevity in animal models (12,13): the *PAX2* age-1 gene codes for phosphatidylinositol-3-kinase in *Caenorhabditis elegans* (14) and the Forkhead box class O (*FOXO*) involved in insulin regulation of glucose production in mammals (15–19). Many genes that are correlated with longevity remain to be identified, but an interesting common feature of the *PAX2* and *FOXO* genes is their involvement in metabolism.

Most of the energy needed to ensure heart function comes from oxidative phosphorylation (OXPHOS) in mitochondria. During this process, electrons are transferred by complexes I–IV of the electron transport chain, whereas protons are translocated into the intermembrane space. The proton gradient generated is utilized by the phosphorylation system to produce ATP. Oxygen is the final electron acceptor and is incorporated into water. As a side product of OXPHOS, reactive oxygen species are released and can cause damage to macromolecules that is suggested to contribute to aging (20). Mitochondrial defects associated with aging have been characterized in isolated mitochondria from the F344 heart (21–24). The OXPHOS defects were localized in the interfibrillar mitochondria (IFM) (21), located between the myofibrils (25), and involved a decrease in activities of complexes III (26,27) and IV (21). According to Suh and colleagues (28), the defect in the IFM involved a decrease in reductive capacity and an increase in oxidative stress.

In our study, we investigated mitochondrial function in cardiac permeabilized fibers from male young adults and elderly (age of 50% mortality) from three different strains

of rats: the F344, the BN, and the hybrid F344×BN. The objective was to correlate the cardiac aging mitochondrial defect with the aging phenotypes, that is, longevity, in the three strains of rats. The three strains were chosen for their importance as aging models and for their difference in sensitivity to aging lesions (10,29). Cardiomyopathy lesions occurred in about 90%–100% of the F344 rats (29), whereas it is present in 63% of the BN and hybrids (10). Heart enlargement is more frequent in the BN compared with the hybrids (10).

Mitochondrial dysfunction is pronounced in the cardiac permeabilized fibers from the F344, complementing data previously obtained in isolated mitochondria. Furthermore, our results show for the first time a correlation between the severities of the aging phenotype in the heart of different strains of rat. Mitochondrial function tends to decrease with aging in the BN, whereas the hybrids F344×BN, which have a longer life span and the lowest rate of age-related pathology, showed completely normal mitochondrial function in the elderly. These results suggest that mitochondrial dysfunction not only accompanies aging but also contributes to the decline in cardiac function during aging.

Methods

Animals

Male F344, BN, and hybrids F344×BN were obtained from Harlan Sprague Dawley, Inc. (Indianapolis, IN), through an agreement with the National Institutes on Aging. The rats were killed in the morning by decapitation and studied at 7.3 ± 1.6 and 24.4 ± 0.9 months of age for the F344, 6.3 ± 0.7 and 31.6 ± 1.0 months of age for the BN, and 6.0 ± 0.0 and 31.0 ± 0.0 for the hybrids. The age of the rats was calculated from the date of birth. The older group of rats were at the age where approximately 50% mortality occurred (10). All procedures were approved by the Department of Veterans Affairs and the Case Western Reserve University Institutional Animal Care and Use Committee and performed in accordance with the National Institutes of Health guidelines for care and use of animals in research.

Preparation of Permeabilized Myocardial Fibers

Approximately 50 mg of cardiac apex was removed from each heart and transferred into 2.5 mL of ice-cold relaxing solution containing 2.77 mM CaK_2 ethylene glycol tetraacetic acid (EGTA), 7.23 mM K_2EGTA, 20 mM immidazole, 20 mM taurine, 6.56 mM $MgCl_2$, 5.77 mM ATP, 15 mM phosphocreatine, 0.5 mM dithiothreitol, and 50 mM K-MES (pH 7.1 at 0°C). After rapid dissection of the myocardial tissue, bundles of fibers were permeabilized by gentle agitation for 30 minutes at 4°C in the relaxing solution supplemented with 50 μg/mL saponin (30,31). Fibers were washed for 10 minutes by agitation in ice-cold mitochondrial respiration medium MIR05 containing 110 mM sucrose, 60 mM K-lactobionate, 0.5 mM EGTA, 1 g/l bovine serum albumin fatty acid free, 3 mM $MgCl_2$, 20 mM taurine, 10 mM KH_2PO_4, and 20 mM K-N-2hydroxyethylpiperazine-N-2-ethanesulponate (HEPES) (pH 7.1) (32); blotted; weighed; and immediately used for respirometric measurements.

High-Resolution Respirometry

Respiration was measured at 37°C with 1.5–3.0 mg of permeabilized fibers per respiration chamber [OROBOROS Oxygraph 2k, Innsbruck, Austria (33)] containing 2 mL of MIR05. Datlab software (OROBOROS Instruments) was used for data acquisition and analysis. For each heart, replicate measurements were performed; the data are presented as mean and SD of all the replicate measurements for five young and five old F344 hearts, seven young and six old BN hearts, and three young and three old hybrid F344×BN hearts.

The first protocol used for evaluating mitochondrial function is presented in Figure 1A. The following substrates, uncoupler, and inhibitors were added (final concentration in the chamber): glutamate (10 mM), malate (5 mM), ADP (2.5 mM), cytochrome *c* (cyt. *c*; 10 μM), succinate (10 mM), dinitrophenol (DNP; titration up to an optimum concentration, 5–20 μM), rotenone (0.5 μM), antimycin A (2.5 μM), ascorbate (2 mM), tetramethylphenylenediamine (TMPD; 0.5 mM), and azide (15 mM). A lower than 7% increase of respiration was observed after addition of cytochrome *c*, supporting the integrity of the outer mitochondrial membrane (Figure 1). Mitochondrial respiration was corrected for oxygen flux due to instrumental background and for residual oxygen consumption (*ROX*) after inhibition of complexes I, II, and III with rotenone and antimycin A (34,35). For complex IV respiration (ascorbate + TMPD), the background measured in the presence of azide was subtracted. Respiratory flux was expressed in picomole O_2 per second per milligram wet weight of fibers. A second experiment was performed with a low oxygen level (60 nmol/mL) in the young and old F344 cardiac fibers in the presence of glutamate + malate + saturating ADP.

In the F344 rat hearts, a subsequent experiment (Figure 2A) was used to evaluate respiration though complex III using duroquinol (1 mM) as the substrate in the presence of rotenone (0.5 μM) before and after addition of ADP (2.5 mM).

Citrate Synthase Activity

The contents of the respiration chamber were removed after the OXPHOS measurement, and the chamber was rinsed twice with 500 μL MIR05. The fibers were homogenized on ice with 20 passes in a 2-mL glass homogenizer (Kontes Glass Co., Vineland, NJ) and frozen for subsequent determination of citrate synthase (CS) activity using a diode array spectrophotometer at 412 nm (36).

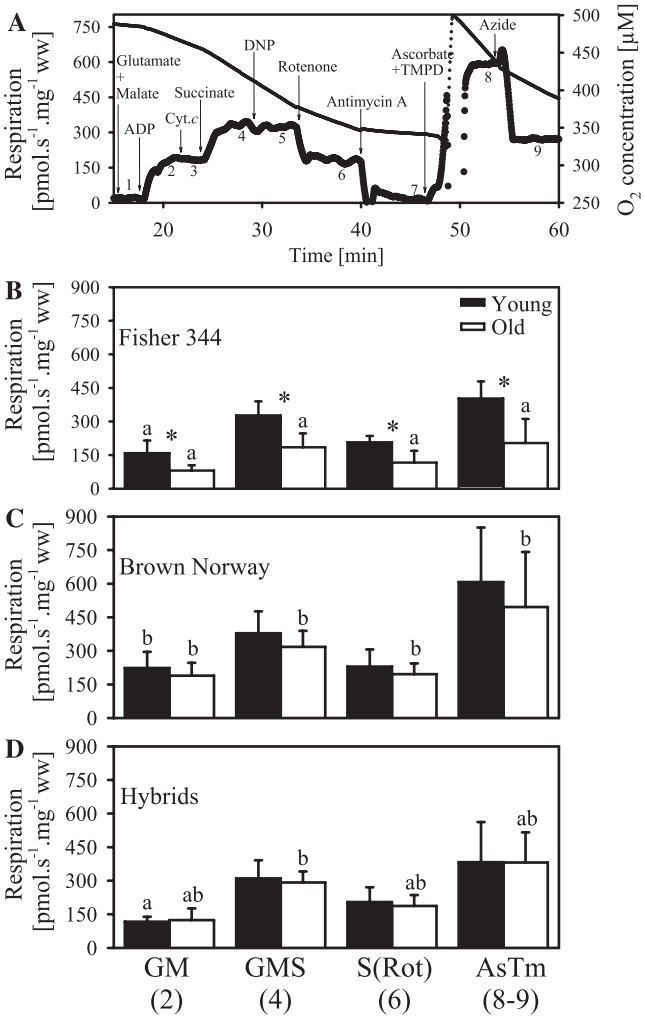

Figure 1. Mitochondrial respiration in cardiac permeabilized fibers from young and old Fisher 344, Brown Norway, and hybrid Fisher 344×Brown Norway. (**A**) Representative experiments with permeabilized fibers from 6-month Fisher 344 rat cardiac fibers with a multiple titration protocol. The traces represent the oxygen consumption (left axis, bold line) and oxygen concentration (right axis, thin line) as a function of time. The multiple titration protocol (representative experiment) comprised the following steps: (a) resting respiration in the presence of glutamate + malate (GM) without ADP, (b) coupled respiration in the presence of GM, after addition of saturating ADP, (c) addition of cytochrome *c* to test for integrity of outer mitochondrial membrane, (d) succinate to measure respiration in the presence of GMS, (e) uncoupling with DNP (no effect), (e) succinate-supported oxidation after inhibition of complex I with rotenone [S(Rot)], (f) residual oxygen consumption after inhibition of complex III with antimycin A, (g) complex IV respiration in the presence of ascorbate + TMPD (AsTm), (h) inhibition of complex IV with azide. Arrows indicate times of titrations of the substrates, uncoupler, and inhibitors. (**B**, **C**, and **D**) Mean ± SD for coupled mitochondrial respiration in the presence of ADP in cardiac permeabilized fibers from young and old Fisher 344 (**B**), Brown Norway (**C**), and hybrid Fisher 344×Brown Norway rats (**D**). The data are with GM (Step 2 in **A**), GMS (Step 4 in **A**), S(Rot) (Step 6 in **A**), and AsTm (Step 8 minus 9 in **A**). The asterisk indicates significant differences between age groups for the same state and strain. The letters indicate differences between strains for the same age and state; bars with either no letter or with one similar letter are not significantly different.

Electron Microscopy

Specimens of the cardiac apex and freshly prepared permeabilized fibers were fixed for transmission electron microscopy. Heart specimens were immediately fixed by immersion in triple aldehyde-dimethyl sulfoxide mixture of Kalt and Tandler (37). The permeabilized fibers in MIR05 were mixed 1:1 with quarter strength Karnovsky's fixative prepared with HEPES buffer (final Karnovsky fixative concentration 1:8). After rinsing in distilled water, all specimens were postfixed in ferrocyanide-reduced osmium tetroxide (38). Thin sections were sequentially stained with acidified uranyl acetate (39) followed by Sato's triple lead stain as modified by Hanaichi and colleagues (40) and examined in a JEOL 1200EX electron microscope.

Data Analysis

Statistical analyses were performed using SigmaStat 4 (Aspire Software International, Ashburn, VA). The criteria of normality and the homogeneity of variance for analysis of variance were tested for each variable with Kolmogorov–Smirnov tests (with Lilliefors' correction) and Spearman tests, respectively. For variables meeting these criteria (ADP-stimulated mitochondrial respiration in the presence of glutamate + malate, glutamate + malate + succinate, and glutamate + malate + succinate + rotenone), differences among age groups and strains were tested with two factors analysis of variances (strains and age groups), followed by pairwise comparisons with Tukey's test. For variables that did not meet the criteria (resting respiration, complex IV respiration, CS activity), differences among groups were tested with Kruskal–Wallis tests followed by a posteriori Mann–Whitney comparisons. A *t* test for dependent samples was used to determine the effects of addition of cytochrome *c* and uncoupler. $p < .05$ was considered significant. Results are presented as means ± SD.

Results

Mitochondrial Respiration During Aging

Resting respiration is measured in the presence of glutamate + malate, before addition of ADP, and is usually considered as the oxygen consumption that represents proton leak, electron slip, and proton cycling (41). In permeabilized cardiac fibers, resting respiration (in picomole per second per milligram) is not significantly different between age groups in the F344 (21.5 ± 8.0 and 13.7 ± 4.3 for 6 and 24 months, respectively), in BN (21.3 ± 10.1 and 26.7 ± 12.1 for 6 and 31 months, respectively), nor in hybrids F344×BN (23.4 ± 5.5 and 16.2 ± 5.7 for 6 and 30 months, respectively).

Respiration coupled with the production of ATP is first measured in the presence of substrates feeding electrons into complex I (glutamate + malate) with a saturating concentration of ADP. In permeabilized fibers from the F344 heart, oxidation of glutamate + malate is decreased by about 49% in the aged hearts compared with the adult hearts (Figure 1B). The oxygen consumption by the fibers in the

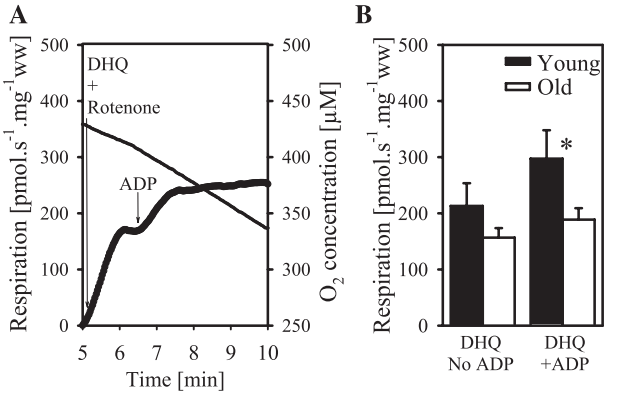

Figure 2. Duroquinol + rotenone oxidation in cardiac permeabilized fibers from young and old Fisher 344 rats. Resting respiration is measured in the presence of duroquinol + rotenone without ADP (DHQ and no ADP). Coupled respiration is measured after the addition of saturating ADP to the DHQ (DHQ and +ADP). (**A**) A representative trace with permeabilized fibers of a 6-month rat. The traces represent the oxygen consumption (left axis, bold line) and oxygen concentration (right axis, thin line) as a function of time. (**B**) Data for the different age groups. The asterisk indicates significant differences between age groups for the same state and strain.

presence of glutamate + malate + ADP at low oxygen level (60 nmol/mL) is decreased by approximately 50% compared with measurement at high air saturation, and the aging defect is observed both at low and at high oxygen levels (results not shown). Coupled respiration is increased by the addition of succinate to glutamate + malate, providing substrates feeding electrons into complexes I and II (CI+II) simultaneously (Figure 1A). Oxidation of glutamate + malate + succinate is decreased by 43% in the permeabilized fibers from the F344 heart with aging (Figure 1B).

Uncoupling with DNP does not increase respiration supported by glutamate + malate + succinate, indicating no limitation of electron transport by the phosphorylation system in the young or in the old rats (Figure 1A). Addition of rotenone inhibits complex I, so the respiration due to the entry of electrons through complex II is measured. Aging also decreases succinate-supported respiration by 44% in the F344 cardiac permeabilized fibers (Figure 1B). After inhibition of complex III with antimycin A, ascorbate and TMPD are added to measure complex IV respiration. As observed for other substrates, complex IV respiration is decreased by 49% in the aged cardiac fibers from the F344 heart (Figure 1B). In a second series of experiments, respiration with duroquinol + rotenone, which provides reducing equivalents to complex III, is measured. Duroquinol-supported resting respiration, before the addition of ADP, does not vary significantly between age groups in F344 rats (Figure 2B). Coupled duroquinol respiration is 37% lower in the 24-month F344 rats compared with the 6-month F344 rats (Figure 2B).

In the BN rats, coupled glutamate + malate respiration decreased by 15% with aging (Figure 1C). Similarly, oxidation of glutamate + malate + succinate, succinate + rotenone, and ascorbate + TMPD shows a decrease with aging of 16%, 15%, and 18%, respectively (Figure 1C). These decreases do not reach significance with any of the substrates but are close with glutamate + malate (p = .165), glutamate + malate + succinate (p = .065), and succinate + rotenone (p = .167).

In the hybrids, similar respiration rates are measured in the young and in the old rat in the presence of all substrates (Figure 1D).

Strains Differences in Mitochondrial Respiration

In the 6-month rat heart fibers, resting respiration does not show any significant differences between the strains. In the old rats, however, resting respiration was significantly lower in the F344 compared with the BN rats (13.7 ± 4.3 and 26.7 ± 12.1 pmol/s/mg, respectively).

In the 6-month rats, coupled ADP-stimulated respiration in the presence of glutamate + malate is higher in the BN than in both F344 and hybrids F344×BN (Figure 1C–E). Oxidation of glutamate + malate + succinate, succinate + rotenone, and ascorbate + TMPD, however, is not significantly different between the strains in the young rats (Figure 1C–E).

Due to the aging defect in the F344 cardiac fibers, respiration with glutamate + malate, glutamate + malate + succinate, succinate + rotenone, and ascorbate + TMPD is significantly lower in the old F344 compared with the old BN rats (Figure 1B and C). The oxidation rates in the permeabilized fibers from the hybrid elderly group are between those in the elderly groups of the two parent strains (Figure 1B–D).

Mitochondrial Content

The mitochondrial content, as evaluated by the activity of CS, is not significantly different between strains or age groups within a strain (Figure 3). However, there is a trend for a decrease in CS activity in the old rats compared with the young rats in the F344 (19% with a p = .080), in the BN (13% with p = .095), and less so in the hybrid rats (10%; Figure 3). When mitochondrial respiration is expressed per unit of CS activity, the aging defect is still present in the F344 rats (results not shown).

Cardiac Ultrastructure

The longitudinal sections of the 6-month (Figure 4A) and 24-month old (Figure 4B) Fischer 344 cardiac tissue clearly show the intactness of the plasma membrane and of the mitochondria. These electron micrographs illustrate the two populations of cardiac mitochondria: subsarcolemmal (SSM) located beneath the plasma membrane and IFM located between the myofibrils. There appears to be pockets of slightly larger mitochondria in the 6-month heart, but this is not consistent.

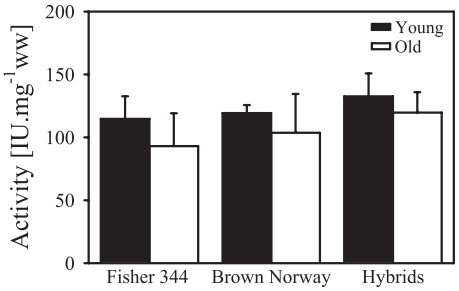

Figure 3. Citrate synthase activity in cardiac permeabilized fibers from young and old Fisher 344, Brown Norway, and Hybrid Fisher 344×Brown Norway rats. Data are mean ± SD.

Permeabilized Fiber Ultrastructure

After dissection and permeabilization of the plasma membrane in the 6-month F344 heart, the SSM maintained their subsarcolemmal position (Figure 4C), even though the plasma membrane has been disrupted. In a like manner, the permeabilized fibers from the 24-month heart show the retention of SSM (Figure 4D). The higher magnification image shows disruption of the plasma membrane in the 6-and the 24-month hearts (Figure 4E and F), indicating that permeabilization has occurred.

The ultrastructure of both mitochondrial populations (SSM and IFM) is preserved after cardiac muscle permeabilization in the 6-month rats (Figure 4C). The outer, inner, and cristae membranes of both populations of mitochondria are well preserved (Figure 4E). Similarly, the permeabilized fibers from the 24-month rats show plasma membrane disruption and intactness of mitochondrial membranes in both SSM and IFM (Figure 4D and F). The SSMs in the permeabilized fibers from the 24-month rat heart have an increase in angulated cristae compared with the 6-month rat (Figure 4F). These angulated cristae are observed only in the SSM population from samples prepared after fiber permeabilization.

Discussion

In order to focus on the role of mitochondrial dysfunction in aging, we studied three strains of rat presenting different aging phenotypes: the F344, the BN, and the hybrids F344×BN. Our study identifies change in mitochondrial function with aging in cardiac permeabilized fibers that varies between rat strains. Our results show a correlation between the impairment of mitochondrial function with aging and the severity of age-related pathologies in the cardiac permeabilized fibers from three strains of rat. The elderly from the three stains are studied at the age at which 50% mortality occurs. The F344 rat is the strain with the shortest life span and the more pronounced age-related pathology (10) and with the greatest impairment of mitochondrial function in aging. Permeabilized cardiac fibers from the elderly show a 37%–49% decrease in respiration compared with the young rat. The BN rats live longer and are less affected by age-related pathology compared with the F344 (10); mitochondrial respiration decreased by 15%–18% with all the substrates in the elderly but did not reach significance. In the hybrid F344×BN, who live longer and healthier lives compared with the BN rats (10), no impairment in mitochondrial oxidation is detected with aging. In

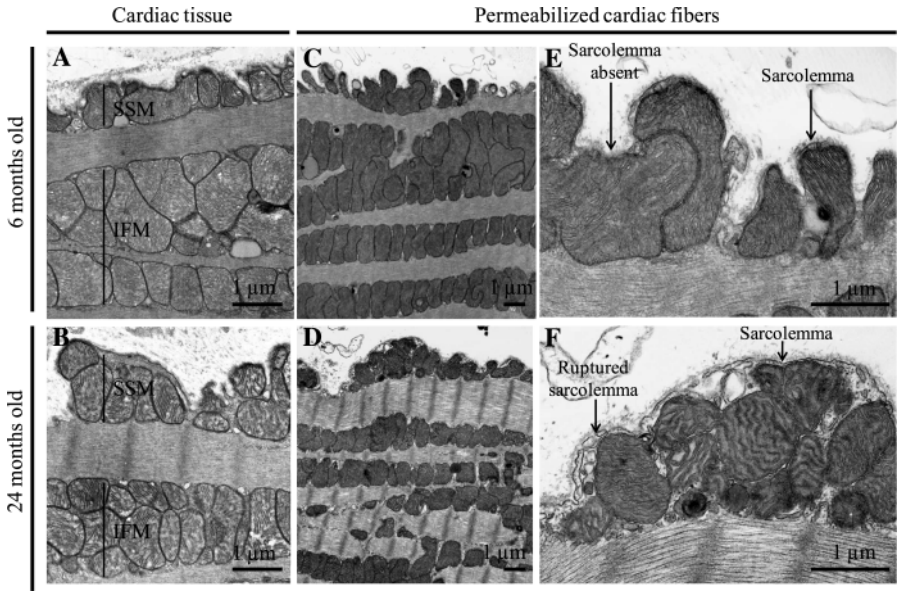

Figure 4. Electron micrographs of the cardiac tissue and permeabilized fibers from young and old Fisher 344 rats: (**A**) 6 months and (**B**) 24 months. The subsarcolemmal (SSM) and interfibrillar (IFM) mitochondria are identified. The ultrastructure of the permeabilized fibers is shown in (**C**) 6 months at low magnification, (**D**) 24 months at low magnification, (**E**) 6 months at low magnification, (**F**) 24 month at high magnification. In the higher magnification micrographs, some segments of the sarcolemma are intact, but others are fragmented; examples are identified with arrows.

the three strains, the mitochondrial content is not significantly different between age groups. The ultrastructure of both the cardiomyocyte muscle and their mitochondria is unaltered with aging in the F344 rats.

The impairment of mitochondrial function in aging observed in the permeabilized fibers from the F344 rats is in agreement with previous results in isolated mitochondria (21–24). In cardiac tissue of the F344 rats, Fannin and colleagues (21) observed a decrease of 25% in the yield of IFM, which displayed a 25% decrease in OXPHOS. This amounts to a total loss in oxidative capacity of 50% in the IFM, with no change in the SSM. Our measurements in permeabilized fibers include both SSM and IFM mitochondria, as confirmed by electron microscopy. As IFM are dominant in fibers, our results are concordant with the previous study using isolated mitochondria (21).

Because the impairment in mitochondrial function in the F344 rats involves the oxidation of glutamate + malate, succinate, duroquinol, and TMPD + ascorbate and feeding electrons into complex I, II, III, and IV, respectively, we addressed the question of whether there is a decrease in the mitochondrial content in the cardiac fibers. CS activity in the fibers, used as a marker of mitochondrial content, is not significantly different between age groups in the F344 heart. These data agree with those of Fannin and colleagues (21) in cardiac muscle homogenate of young and old F344 rats. In both studies, the CS activity is slightly but not significantly lower in the old rats: 19% in our study and 18% in that of Fannin and colleagues (21), ruling out a decrease in mitochondrial content. In the BN rats, the activity of CS also shows a slight but not significant trend between age groups (13% decrease in the old), although the trend is accompanied by high variability in the elderly group, making the biologic relevance of this trend questionable. In the hybrids, CS activity is not significantly different between age groups.

The similarity of CS activity between the age groups in our study argues against an important change in the volume occupied by fibrotic tissues in the cardiomyocytes from old compared with young hearts. As previously reported, aging in the rat heart is associated with left ventricular hypertrophy, changes in ventricle diameter, cardiomyocyte hypertrophy and loss, fibrosis, and collagen deposition, all of which are signs of cardiomyopathy (42–46). In our project, the elderly F344 rats are studied at a time point before these symptoms appear (21,22). Our results clearly show a cardiac OXPHOS aging defect in the F344 rat heart before the occurrence of other cardiac abnormalities, in agreement with our study on isolated mitochondria (21).

The ultrastructure of muscle and of mitochondria is unaltered by aging in the cardiac muscle of F344 rats, as shown by electron microscopy. This is in accord with previous data using transmission (21) and scanning electron microscopy (47). Mitochondrial structure and cristae configuration do not play a major role in age-related cardiac mitochondrial defects in the F344 rat. Electron microscopy of the permeabilized fibers in our study shows a more pronounced cristae angulation in the SSM of the 24-month compared with the 6-month F344 rats; this difference is apparent only in the SSM. Mitochondrial integrity for both populations, however, is well preserved in the permeabilized fibers, as confirmed by electron microscopy.

The mitochondrial defect with aging in the F344 rats, at a minimum, involves complex IV respiration, because TMPD + ascorbate respiration is decreased, as well as all the respiration with other substrates (glutamate + malate, succinate + rotenone, and DHQ + rotenone) which need complex IV as the final electron acceptor. The defect in complex IV respiration measured previously in isolated IFM from aged F344 hearts (21) was explained by an altered inner membrane environment because the defect in cytochrome *c* oxidase in partially permeabilized mitochondria can be reversed by the addition of phospholipid liposomes or by freeze thawing (21,48). Loss of cardiolipin was suggested as the cause of the defect because cytochrome *c* oxidase requires this phospholipid for optimal activity (49–51). This possibility was ruled out by the fact that cardiolipin content is unaltered in aging in both mitochondrial populations in the F344 rat heart (26).

A defect in mitochondrial function is detected in permeabilized fibers, whereas the impairment is present in the IFM. In permeabilized fibers both mitochondrial populations are studied. If oxygen diffuses slowly through the permeabilized fibers, it would first reach the SSM located beneath the plasma membrane and ultimately the IFM located between the myofibrils. A lack of oxygen diffusion into the myofibers would favor respiration in SSM for which the oxygen is less likely to be limiting. The SSM, however, do not present an aging defect in the heart of F344 rats (21,26,27). The experiments were performed at high oxygen (oversaturation) to avoid any artifact due to the problem of oxygen diffusion (52). The aging defect in the F344 strains is observed also when the oxygen drops to one third below air saturation (60 nmol/mL). Our data by showing an aging defect localized in the IFM at both low and high oxygen confirm that the measurements in permeabilized fibers include both mitochondrial populations. The ability to detect the aging defect in permeabilized fibers offers advantages such as the need for a very small amount of tissue (a few milligrams), with the mitochondria being retained in the cellular environment. This approach provides an opportunity to study the human heart despite the small amount of tissues available from routine surgery (53). This is of interest, especially if an aging defect is present.

The only available data for addressing mitochondrial activity with age in the human heart found that the activity of cytochrome *c* oxidase (complex IV) does not change between the ages of 10 days and 67 years, whereas the activity and content of CS increased (54). These enzyme activity data in the human heart have not been confirmed; in

addition what is needed are data on mitochondrial respiration. In the rats, a decrease in complex IV respiration is observed in the F344, but none of the strains show an increase in CS activity with aging, raising a question as to whether the hybrid F344×BN is a superior model for the age-associated changes seen in human cardiac muscle (55,56).

In conclusion, our study shows that the age-associated mitochondrial oxidation defect in cardiac fibers is strain specific, is positively correlated with the severity of the aging-related pathologies, and is inversely correlated with the life span. The F344 rat has a short life span and a ~45% decrease in mitochondrial oxidation in the permeabilized cardiac fibers from the old rat compared with the young rat. Compared with the F344, the BN rats live longer and have a consistent 15%–18% loss of mitochondrial respiration with all the substrates used in the elderly heart compared with the young heart. This trend does not reach significance. In hybrids, more resistant to aging than are the BN and F344 rats, mitochondrial function is preserved during aging. Because the mitochondrial oxidation defect in the F344 occurred at a time point preceding morphological impairment of the cardiac tissue, mitochondrial dysfunction seems to be a contributor to the aging phenotype observed in the F344 rats. The mitochondrial defect constitutes a potential target for implementation of therapeutic treatment (57–59). As an example, products such as acetylcarnitine that activates mitochondrial biogenesis, presumably by acetylation of mitochondrial proteins (60), are of interest. Elucidation of the mechanism of action of such compounds would offer promising avenues in the therapy of heart disease. Our results highlight mitochondrial dysfunction as a contributing factor to the aging process in the heart. Furthermore, the use of permeabilized fibers to detect the aging defect in our study provides a method easily transferable to the study of the aging defect in the human heart.

Funding

This work was supported by a Program Project Grant (2P01 AG015885). H.L. is supported by a fellowship from the National Sciences and Engineering Research Council of Canada.

Acknowledgment

We thank Dr. Bernard Tandler for discussion and editorial comments.

References

1. Lakatta EG, Sollott SJ. The "heartbreak" of older age. *Mol Interv*. 2002;2:431–446.
2. Terman A, Brunk UT. Aging as a catabolic malfunction. *Int J Biochem Cell Biol*. 2004;36:2365–2375.
3. Lakatta EG, Levy D. Arterial and cardiac aging: major shareholders in cardiovascular disease enterprises: Part I: aging arteries: a "set up" for vascular disease. *Circulation*. 2003;107:139–146.
4. Lakatta E. Aging effects on the vasculature in health: risk factors for cardiovascular disease. *Am J Geriatr Cardiol*. 1994;3:11–17.
5. Barzilai N, Shuldiner AR. Searching for human longevity genes: the future history of gerontology in the post-genomic era. *J Gerontol Med Sci*. 2001;56:M83–M87.
6. Atzmon G, Schechter C, Greiner W, Davidson D, Rennert G, Barzilai N. Clinical phenotype of families with longevity. *J Am Geriatr Soc*. 2004; 52:274–277.
7. Perls TT, Wilmoth J, Levenson R, et al. Life-long sustained mortality advantage of siblings of centenarians. *Proc Natl Acad Sci USA*. 2002;99:8442–8447.
8. Weindruch R, Masoro E. Concerns about rodent models for aging research. *J Gerontol*. 1991;46:B87–B88.
9. Tanaka S, Shito A, Tamaya N, Miyaishi O, Nishimura M, Ohno T. Difference in average survival between F344/Du and F344/N rats is not due to genetic contamination. *Arch Gerontol Geriatr*. 2002;34:19–28.
10. Lipman RD, Chrisp CE, Hazzard DG, Bronson RT. Pathologic characterization of brown Norway, brown Norway x Fischer 344, and Fischer 344 x brown Norway rats with relation to age. *J Gerontol Biol Sci*. 1996;51:B54–B59.
11. Perls T, Terry D. Genetics of exceptional longevity. *Exp Gerontol*. 2003;38:725–730.
12. Partridge L, Gems D. Mechanisms of ageing: public or private? *Nat Rev Genet*. 2002;3:165–175.
13. Longo VD, Finch CE. Evolutionary medicine: from dwarf model systems to healthy centenarians? *Science*. 2003;299:1342–1346.
14. Friedman DB, Johnson TE. A mutation in the age-1 gene in Caenorhabditis elegans lengthens life and reduces hermaphrodite fertility. *Genetics*. 1988;118:75–86.
15. Nakae J, Kitamura T, Silver DL, Accili D. The forkhead transcription factor Foxo1 (Fkhr) confers insulin sensitivity onto glucose-6-phosphatase expression. *J Clin Invest*. 2001;108:1359–1367.
16. Ayala JE, Streeper RS, Desgrosellier JS, et al. Conservation of an insulin response unit between mouse and human glucose-6-phosphatase catalytic subunit gene promoters: transcription factor FKHR binds the insulin response sequence. *Diabetes*. 1999;48:1885–1889.
17. Durham SK, Suwanichkul A, Scheimann AO, et al. FKHR binds the insulin response element in the insulin-like growth factor binding protein-1 promoter. *Endocrinology*. 1999;140:3140–3146.
18. Hall RK, Yamasaki T, Kucera T, Waltner-Law M, O'Brien R, Granner DK. Regulation of phosphoenolpyruvate carboxykinase and insulin-like growth factor-binding protein-1 gene expression by insulin. The role of winged helix/forkhead proteins. *J Biol Chem*. 2000;275:30169–30175.
19. Nadal A, Marrero PF, Haro D. Down-regulation of the mitochondrial 3-hydroxy-3-methylglutaryl-CoA synthase gene by insulin: the role of the forkhead transcription factor FKHRL1. *Biochem J*. 2002;366:289–297.
20. Beckman KB, Ames BN. The free radical theory of aging matures. *Physiol Rev*. 1998;78:547–581.
21. Fannin SW, Lesnefsky EJ, Slabe TJ, Hassan MO, Hoppel CL. Aging selectivity decreases oxidative capacity in rat heart interfibrillar mitochondria. *Arch Biochem Biophys*. 1999;372:399–407.
22. Lesnefsky EJ, Gudz TI, Moghaddas S, et al. Aging decreases electron transport complex III activity in heart interfibrillar mitochondria by alteration of the cytochrome c binding site. *J Mol Cell Cardiol*. 2001;33:37–47.
23. Lesnefsky EJ, Moghaddas S, Tandler B, Kerner J, Hoppel CL. Mitochondrial dysfunction in cardiac disease: ischemia-reperfusion, aging, and heart failure. *J Mol Cell Cardiol*. 2001;33:1065–1089.
24. Moghaddas S, Hoppel CL, Lesnefsky EJ. Aging defect at the Q_O site of complex III augments oxyradical production in rat heart interfibrillar mitochondria. *Arch Biochem Biophys*. 2003;414:59–66.
25. Palmer JW, Tandler B, Hoppel CL. Biochemical properties of subsarcolemmal and interfibrillar mitochondria isolated from rat cardiac muscle. *J Biol Chem*. 1977;252:8731–8739.
26. Moghaddas S, Stoll MS, Minkler PE, Salomon RG, Hoppel CL, Lesnefsky EJ. Preservation of cardiolipin content during aging in rat heart interfibrillar mitochondria. *J Gerontol Biol Sci*. 2002;57:B22–B28.
27. Lesnefsky EJ, He D, Moghaddas S, Hoppel CL. Reversal of mitochondrial defects before ischemia protects the aged heart. *FASEB J*. 2006;20:1543–1545.

28. Suh JH, Heath SH, Hagen TM. Two subpopulations of mitochondria in the aging rat heart display heterogenous levels of oxidative stress. *Free Radic Biol Med*. 2003;35:1064–1072.
29. Maeda H, Gleiser CA, Masoro EJ, Murata I, McMahan CA, Yu BP. Nutritional influences on aging of Fischer 344 rats: II. Pathology. *J Gerontol*. 1985;40:671–688.
30. Kuznetsov AV, Schneeberger S, Seiler R, et al. Mitochondrial defects and heterogeneous cytochrome *c* release after cardiac cold ischemia and reperfusion. *Am J Physiol Heart Circ Physiol*. 2004;286: H1633–H1641.
31. Veksler VI, Kuznetsov AV, Sharov VG, Kapelko VI, Saks VA. Mitochondrial respiratory parameters in cardiac tissue: a novel method of assessment by using saponin-skinned fibers. *Biochim Biophys Acta*. 1987;892:191–196.
32. Gnaiger E, Kuznetsov AV, Schneeberger S, et al. Mitochondria in the cold. In: Heldmaier G, Klingenspor M, eds. *Life in the Cold*. Heidelberg, Germany: Springer; 2000:431–442.
33. Gnaiger E. Polarographic oxygen sensors, the oxygraph and high-resolution respirometry to assess mitochondrial function. In: Dykens JA, Will Y, eds. *Mitochondrial Dysfunction in Drug-Induced Toxicity*. New York: John Wiley; 2008:327–352.
34. Gnaiger E, Lassnig B, Kuznetsov A, Reiger G, Margreiter R. Mitochondrial oxygen affinity, respiratory flux control and excess capacity of cytochrome *c* oxidase. *J Exp Biol*. 1998;201:1129–1139.
35. Gnaiger E, Steinlechner-Maran R, Méndez G, Eberl T, Margreiter R. Control of mitochondrial and cellular respiration by oxygen. *J Bioenerg Biomemb*. 1995;27:583–596.
36. Matsuoka Y, Srere PA. Kinetic studies of citrate synthase from rat kidney and rat brain. *J Biol Chem*. 1973;248:8022–8030.
37. Kalt MR, Tandler B. A study of fixation of early amphibian embryos for electron microscopy. *J Ultrastruct Res*. 1971;36:633–645.
38. Karnovsky MJ. Use of ferrocyanide-reduced osmium tetroxide in electron microscopy. In: Proceedings of 11th Annual Meeting of the American Society of Cell Biology. November 15–17, 1971; New Orleans, LA. 146.
39. Tandler B. Improved uranyl acetate staining for electron microscopy. *J Electron Microsc Tech*. 1990;16:81–82.
40. Hanaichi T, Sato T, Iwamoto T, Malavasi-Yamashiro J, Hoshino M, Mizuno N. A stable lead by modification of Sato's method. *J Electron Microsc*. 1986;35:304–306.
41. Brand MD, Chien LF, Ainscow EK, Rolfe DF, Porter RK. The causes and functions of mitochondrial proton leak. *Biochim Biophys Acta*. 1994;1187:132–139.
42. Anversa P, Palackal T, Sonnenblick EH, Olivetti G, Meggs LG, Capasso JM. Myocyte cell loss and myocyte cellular hyperplasia in the hypertrophied aging rat heart. *Circ Res*. 1990;67:871–885.
43. Capasso JM, Fitzpatrick D, Anversa P. Cellular mechanisms of ventricular failure: myocyte kinetics and geometry with age. *Am J Physiol*. 1992;262:H1770–H1781.
44. Capasso JM, Palackal T, Olivetti G, Anversa P. Severe myocardial dysfunction induced by ventricular remodeling in aging rat hearts. *Am J Physiol*. 1990;259:H1086–H1096.
45. Anversa P, Hiler B, Ricci R, Guideri G, Olivetti G. Myocyte cell loss and myocyte hypertrophy in the aging rat heart. *J Am Coll Cardiol*. 1986;8:1441–1448.
46. Anversa P, Kajstura J, Olivetti G. Myocyte death in heart failure. *Curr Opin Cardiol*. 1996;11:245–251.
47. Riva A, Tandler B, Lesnefsky EJ, et al. Structure of cristae in cardiac mitochondria of aged rat. *Mech Ageing Dev*. 2006;127:917–921.
48. Paradies G, Ruggiero FM, Dinoi P, Petrosillo G, Quagliariello E. Decreased cytochrome oxidase activity and changes in phospholipids in heart mitochondria from hypothyroid rats. *Arch Biochem Biophys*. 1993;307:91–95.
49. Vik SB, Capaldi RA. Lipid requirements for cytochrome c oxidase activity. *Biochemistry*. 1977;16:5755–5759.
50. Hoch FL. Cardiolipins and biomembrane function. *Biochim Biophys Acta*. 1992;1113:71–133.
51. Powell GL, Knowles PF, Marsh D. Spin-label studies on the specificity of interaction of cardiolipin with beef heart cytochrome oxidase. *Biochemistry*. 1987;26:8138–8145.
52. Gnaiger E. Capacity of oxidative phosphorylation in human skeletal muscle. New perspectives of mitochondrial physiology. *Int J Biochem Cell Biol*. 2009;41:1837–1845.
53. Lemieux H, Hoppel CL. Mitochondria in the human heart. *J Bioenerg Biomembr*. 2009;41:99–106.
54. Marin-Garcia J, Ananthakrishnan R, Goldenthal MJ. Human mitochondrial function during cardiac growth and development. *Mol Cell Biochem*. 1998;179(1–2):21–26.
55. Hacker TA, McKiernan SH, Douglas PS, Wanagat J, Aiken JM. Age-related changes in cardiac structure and function in Fischer 344 x Brown Norway hybrid rats. *Am J Physiol Heart Circ Physiol*. 2006;290: H304–H311.
56. Rice KM, Linderman JK, Kinnard RS, Blough ER. The Fischer 344/NNiaHSd X Brown Norway/BiNia is a better model of sarcopenia than the Fischer 344/NNiaHSd: a comparative analysis of muscle mass and contractile properties in aging male rat models. *Biogerontology*. 2005;6:335–343.
57. Ventura-Clapier R, Mettauer B, Bigard X. Beneficial effects of endurance training on cardiac and skeletal muscle energy metabolism in heart failure. *Cardiovasc Res*. 2007;73:10–18.
58. Ashrafian H, Frenneaux MP, Opie LH. Metabolic mechanisms in heart failure. *Circulation*. 2007;116:434–448.
59. Finck BN, Kelly DP. Peroxisome proliferator-activated receptor gamma coactivator-1 (PGC-1) regulatory cascade in cardiac physiology and disease. *Circulation*. 2007;115:2540–2548.
60. Rosca MG, Lemieux H, Hoppel CL. Mitochondria in the elderly: is acetylcarnitine a rejuvenator? *Adv Drug Deliv Rev*. 2009;61: 1332–1342.